[PROC. OF JSCE Structural Eng. /Earthquake Eng. Vol. 2, No. 1 April 1985]

NONLNEAR BEHAVIOUR OF CURVED GIRDER-WEB CONSIDERED FLANGE RIGIDITIES

By Katashi FUJII and Hiroshi OHMURA***

The web of thin walled curved girder deflects out of surface by bending moment because of it's curvature. This deflection causes the deformation of the cross section of the curved girder, by which the behaviour of curved girders will be complicated.

In this paper, the part of curved girders between vertical stiffeners was analysed, regarded as sectoral plates and cylindrical shell panel structure. The interaction of flanges and web panel was also considered and evaluated.

Several numerical examples show that the deformation of curved I-girders is affected by tosional behaviour of the flange besides shell action of the web.

1. INTRODUCTION

The behaviour of curved girders is remarkably affected not only by geometric nonlinearity but also by the deformation of the cross section. That is, the web of thin walled curved girders deflects out of plane in bending of the girders, and causes the deformations of the cross section of the girders. Thus the behaviour of curved girders becomes more complicated. Therefore, the behaviour of the deformations of the curved girder-web is very important for the purpose of elucidation of the curved girder behaviour.

The Japanese Specification for Highway Bridge[1] does not provide the requirement for the width / thickness ratio of the web of curved girders, therefore the general standard of the plate girder-web is applied to the design of curved girder-web[6]. This standard for plate girder-web is based on an assumption that the buckling of the web should not occur before yielding in bending and shear. Although there is, indeed, an investigation of curved girder-web as buckling problem[2], the web of curved girders should not be estimated as buckling problem but as displacement problem, because the web deflects out of plane with geometric nonlinearity.

The nonlinear behaviour of webs of curved girders in bending has been investigated by Dabrowski & Wachowiak[3] Culver & Dym[4),5)], Mikami, Furunishi & Yonezawa[6], Kuranishi & Hiwatashi[7]. In these investigations, the web panel with boundaries of flanges and vertical stiffeners was analysed as a cylindrical panel that the deflection along two opposite sides was constrained. However, this analytical model is insufficient to evaluate the practical behaviour of the curved girder-web, because the deflection of the cylindrical panel is constrained along flange-web connections. Namely, the torsional moment is not able to be considered correctly in the analysis, and the web is obviously influenced by the flexural rigidity of the

* Member of JSCE, M. Eng, Research Associate, Hiroshima University (Higashihiroshima).
** Member of JSCE, Dr. Eng, Professor, Hiroshima University.

flange-plate.

In this study, the geometrical nonlinear behaviour of the structural part of curved I-girder between vertical stiffeners is analysed by finite element method as the structure constructed of sectoral plates and a cylindrical shell panel. And the bending condition is assumed in order to compare with the results of previous investigations[3)~7)].

When the plate and shell structure analysis said above is performed, the following alternative conditions are generally assumed as the boundary or load condition on the end cross section of the analytical part. For example in bending, the triangular distribution of normal stress equivalent to the bending moment is assumed, or the triangular distribution of circumferential displacement corresponding to the deflection angle is assumed. Both conditions bring out same results of the displacement and normal stress in the linear analysis of plate girders. But as for curved girders, either the displacement or normal stress does not become triangular distribution[7)]. The latter condition is based on the assumption of displacement field of beams, and attaching importance to the compatibility of displacement between the end cross section of analytical part and that of adjoining part, this condition is concluded to be appropriate in correspondence between analytical models and practical girders. Therefore, adopting the assumption of displacement field of beams, the unknown displacements of a nodal point on the end cross section of the analytical part are expressed by the displacements of the shear center. By this way, the compatibility of displacement at the boundary is automatically satisfied without correcting the each nodal displacements on the end cross section. Moreover the deformation analysis corresponding to arbitrary states of sectional forces in curved girders can be performed, because load data for input is sectional forces of the beam itself.

In the following, the parametric analysis about the deformation of the cross section of curved I-girders in bending is performed. Then behaviours and stresses of the web are investigated in the interaction of flange and web, and the results are compared with the analytical model considered only web panel, in which deflection is constrained along boundary edges.

2. DEFORMATION ANALYSIS AS PLATE AND SHELL STRUCTURE

(1) Sectoral plate element and cylindrical shell element

Curved girders are regarded as the structure that is constructed of sectoral plates and cylindrical shell panels. Then, the sectoral plate element and cylindrical shell element are profitable in the finite element analysis, moreover it is desirable that the rigid body movements and rotations are correctly estimated in these elements. Though cylindrical shell element which shows rigid body movements and rotations correctly has been provided by Cantin&Clough[8)] or Megard[9)], sectral plate element has not been provided.

The displacement function which shows correct rigid body movements and rotations is adopted for the sectoral plate element as well as cylindrical shell element in the analysis. As the approaches to finite element formulation based on incremental theory was already performed[10)], only the displacement function is shown here.

Cylindrical coordinate (r,θ,z) and displacements $(u,v,w,\phi_r,\phi_\theta,\phi_z)$ is shown in **Fig. 1** (a), (b) for sectoral plate element and cylindrical shell element respectively. The displacement functions of respective elements are assumed as follows.

a) Cylindrical shell element

$$u=\alpha_2\sin\beta\eta+\alpha_3\cos\beta\eta+\alpha_4 R\sin\beta\eta-\alpha_5\, a\,\xi\,\beta\eta+\alpha_6\, a\xi\sin\beta\eta+\frac{1}{2}(\alpha_{16}\xi^2+\alpha_{17}\xi\eta$$
$$+\alpha_{18}\eta^2+\alpha_{19}\xi^3+\alpha_{20}\xi^2\eta+\alpha_{21}\xi\eta^2+\alpha_{22}\eta^3+\alpha_{23}\xi^3\eta+\alpha_{24}\xi\eta^3) \qquad (1\cdot a)$$

$$v=\alpha_2\cos\beta\eta-\alpha_3\sin\beta\eta+\alpha_4 R(\cos\beta\eta-1)+\alpha_5\, a\xi\sin\beta\eta$$
$$+\alpha_6\, a\xi\cos\beta\eta+\frac{1}{2}(\alpha_8\xi+\alpha_9\eta+\alpha_{11}\xi\eta) \qquad (1\cdot b)$$

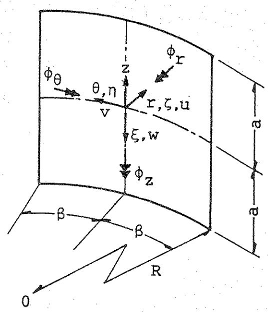

(a) Cylindrical shell element

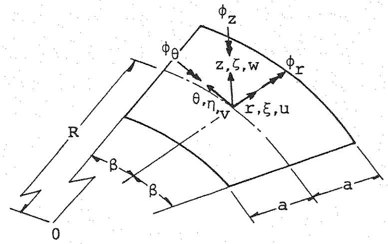

(b) Sectoral plate element

Fig. 1 Finite elements.

$$w=\alpha_1+\alpha_5 R(\cos\beta\eta-1)-\alpha_6 R\sin\beta\eta+\frac{1}{2}(\alpha_7\xi+\alpha_8\eta+\alpha_{10}\xi\eta+\alpha_{12}\eta^2$$

$$+\alpha_{13}\xi\eta^2+\alpha_{14}\eta^3+\alpha_{15}\xi\eta^3) \quad \cdots\cdots (1\cdot c)$$

$$\xi=-z/a \quad \cdots\cdots (1\cdot d)$$

$$\eta=\theta/\beta \quad \cdots\cdots (1\cdot d)$$

b) Sectoral plate element

$$u=\alpha_1\cos\beta\eta+\alpha_2\sin\beta\eta-\alpha_6 R\sin\beta\eta+\frac{1}{2}(\alpha_7\xi+\alpha_8\eta+\alpha_{10}\xi\eta+\alpha_{12}\eta^2$$

$$+\alpha_{13}\xi\eta^2+\alpha_{14}\eta^3+\alpha_{15}\xi\eta^3) \quad \cdots\cdots (2\cdot a)$$

$$v=-\alpha_1\sin\beta\eta+\alpha_2\cos\beta\eta+\alpha_6(r-R\cos\beta\eta)+\frac{1}{2}(\alpha_8\xi+\alpha_9\eta+\alpha_{11}\xi\eta) \quad \cdots\cdots (2\cdot b)$$

$$w=\alpha_3+\alpha_4 r\sin\beta\eta+\alpha_5(R-r\cos\beta\eta)+\frac{1}{2}(\alpha_{16}\xi^2+\alpha_{17}\xi\eta+\alpha_{18}\eta^2+\alpha_{19}\xi^3$$

$$+\alpha_{20}\xi^2\eta+\alpha_{21}\xi\eta^2+\alpha_{22}\eta^3+\alpha_{23}\xi^3\eta+\alpha_{24}\xi\eta^3) \quad \cdots\cdots (2\cdot c)$$

$$\xi=(r-R)/a \quad \cdots\cdots (2\cdot d)$$

$$\eta=\theta/\beta \quad \cdots\cdots (2\cdot d)$$

In equtions (1·a), (1·c), the coefficients α_4 and α_5 are different from those of Cantin&Clough's[8]. This difference is caused by taking the rotational axis in the tangent plane on the $(\xi,\eta)=(0,0)$.

In order to consider the lateral buckling, the nonlinear term for in-plane displacement of r-direction is adopted as well as the term of out-plane deflection.

(2) Treament of the end cross section of the analytical part model

When the deformation analysis is performed about the part of curved I-girders between vertical stiffeners, the displacements and sectional forces must be corresponding to the practical curved girder. Namely, as for displacements, considering the compatibility between the end cross section of the analytical part and that of adjoining part, the displacements on the end cross section are desirable to be satisfied with the displacement field of beams. Kuranishi&Hiwatashi[7] analysed the web panel of curved girders in bending, and the triangular distribution of tangential displacement on the end was prescribed, then the trial and error correction of displacements was performed in order to eliminate the nonlinear normal force depending on girder deflection.

This compatibility is assumed to be satisfied in this analysis. But it was expected to be difficult in convergence to amend the displacements of each nodal point on the end cross section so that the bending moment, torque, shearing force and warping moment might satisfy the required conditions on the end cross section, because not only web but also flange must be considered. Therefore, the displacements of each nodal point on the end cross section are expressed by the displacements of shear center in the end cross section, according to the assumption of displacement field of beams. That is, the 6-displacements of the arbitary point-i on the end cross section (Fig. 2) are calculated from the 7-displacelents of the shear center which are 6-dispacements shown in Fig. 2 and rate of twist.

Now, the displacements of the arbitrary point-i on the end cross section are written by displacements of shear center as follows,

$$\begin{Bmatrix} u_i \\ v_i \\ w_i \\ \phi_{\theta i} \\ \phi_{ri} \\ \phi_{zi} \end{Bmatrix} = \begin{pmatrix} 1 & 0 & 0 & z_s - z_i^* & 0 & 0 & 0 \\ 0 & 1 & 0 & 0 & z_s - z_i & r_s - r_i & -\omega \\ 0 & 0 & 1 & r_i - r_s & 0 & 0 & 0 \\ 0 & 0 & 0 & 1 & 0 & 0 & 0 \\ 0 & 0 & 0 & 0 & 1 & 0 & r_s(r_i - r_s)/r_i \\ 0 & 0 & 0 & 0 & 0 & 1 & -r(z_i - z_s - \omega/r_s)r_i \end{pmatrix} \begin{Bmatrix} u^* \\ v^* \\ w^* \\ \phi_\theta^* \\ \phi_r^* \\ \phi_z^* \\ \psi \end{Bmatrix} \quad \cdots\cdots (3)$$

or

$$\{u_i\} = [t_i]\{u^*\} \quad \cdots\cdots (4)$$

Asterisk * in u^* and ϕ_r^* etc. of Fig. 2 or eq. (3) indicates the shear center. And (r_i, z_j), (r_s, z_s) are the coordinates of point-i and shear center respectively, ω is warping function of flange or web, ψ is the rate of twist $(= \partial\phi_\theta^*/r_s\partial\theta - \partial w^*/r_s^2\partial\theta)$.

On the other hand, the relation between nodal force of point-i and the sectional force is expressed as

$$\{f_i^*\} = [t_i]^T\{f_i\} \quad \cdots\cdots (5)$$

In which $\{f_i^*\}$ is the component of the sectional force caused by nodal force $\{f_i\}$, then, the total of $\{f_i^*\}$ about all nodal points on the end cross section becomes the sectional force of the shear center.

The element stiffeness matrix concerned with the end cross section is transformed as follows.

$$\overset{19\times19}{[K_s]} = [T]^T \overset{24\times24}{[K]} \overset{24\times19}{[T]} \quad \cdots\cdots (6)$$

In eq. (6), $[T]$ is constructed of $\overset{6\times7}{[t_i]}$ and unit matrix $\overset{6\times6}{[E]}$, and $[K]$ is the element stiffeness matrix which includes terms for point-i, but transformed stiffeness matrix $[K_s]$ includes the terms for shear center instead of the terms for point-i. Consequently, the displacements of shear center are analysed by input of sectional forces of the end cross section, and the displacements of point-i are calculated by eq. (4).

(3) Boundary and load conditions

The deformation analysis of practical curved girders has been able to be performed by the way in 2. (2). By the way, in many of the previous investigations, the bending has been chosen as the subject of studies, moreover there are very few reports about web behaviour considered flange rigidities. Therefore, only bending is assumed in this paper in order to compare with the previous reports.

In bending, the boundary and load conditions are considered as follows.

As for displacements, torsion angle ϕ_θ^* and vertical displacement w^* (deflection of the beam) are constrained at the end $(\theta=\alpha)$, and the vertical displacement is constrained at the other end $(\theta=0)$. And as for load conditions, considering the bending moment M_c at the section $\theta=\alpha/2$, the bending moments at the both end are given by $M=M_c\cos\frac{\alpha}{2}$, and the torsional moment $T=M_c\sin\frac{\alpha}{2}$ is given at the end $\theta=0$, (Fig. 3).

The analytical model under these boundary conditions is statically determinate as a beam, therefore torsional moment $T=-M_c\sin\frac{\alpha}{2}$ appears at $\theta=\alpha$ from the equilibrium of the sectional forces. These conditions are called bending state in this paper.

By the way, Nakai, Kitada&Ohminami[11] adopted the boundary condition, that torsion angle at the both ends was constrained, in bending experiments of curved girders. This condition leads to the first order statically indeterminated beam. Though the same results are obtained in linear analysis, the condition of statically indeterminated beam is not adopted in this analysis because it is expected that the bending state may not be satisfied due to torsional moment when the geometric nonlinearity appears remarkably.

For simplicity, the warping of the end cross section is assumed to be free.

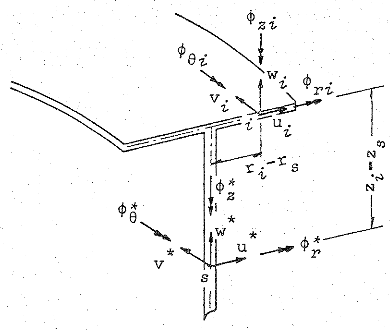

Fig. 2 Displacement relationship between shear center and nodal poist in end cross section.

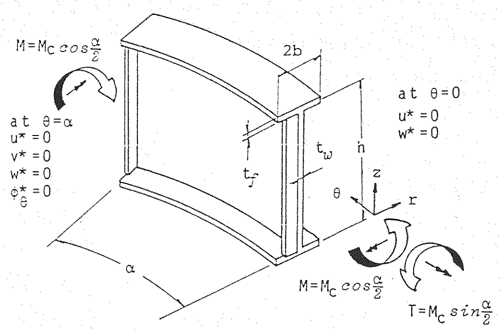

Fig. 3 Load and boundary conditions.

(4) Parameters

It is suggested that the deformation of curved girders is mainly influenced by following parameters $z(=h^2\sqrt{1-\nu^2}/Rt_w)$, h/t_w and $R\alpha/h$ for web, and $b/R, b/t_f, R\alpha/b$ for flange, and as for the interaction of flange and web, $GJ_f/D_wh, EI_f/D_wh, A_{fc}/A_w$. In which, R=radious of the curved girder, α =angle of the analytical part (Fig. 3), h=depth of web, t_w=web thickness, $2b$=flange width, t_f= flange thickness, and GJ_f=torsional rigidity of compressive flange $(=2Gbt_f^3/3)$, $EI_f=2Eb^3t_f/3$, D_w= flexural rigidity of web, and A_{fc}, A_w=the area of compressive flange and web respectively.

Parameter z and GJ_f/D_wh are particularly investigated, because these parameters are expected to affect especially to the deformation of curved girders. The radious of practical curved girders is usually $R>30$ m, and z is generally less than 10, therefore the radious R and parameter z are assumed 300 m$>R>$30 m, $z<15$ respectively. And the ratio b/t_f is assumed $2<b/t_f<24$. In Japanese Specification for Highway Bridge[1], b/t_f is provided as $t/t_f<16$, but in this analysis $b/t_f=24$ is added in order to examine the influence of torsional buckling of comressive flange. h/t_w is assumed as 150 and 300, in order to obtain the remarkable geometric nonlinear behaviour, and $R\alpha/h=1$, $A_{fc}/A_w=0.5$, 1.0 are also assumed. Depending on h/t_w or b/t_f, GJ_f/D_wh and EI_f/D_wh change to $1.5<GJ_f/D_wh<90$, $1\,200<EI_f/D_wh<10\,000$.

Bendirg moment is indicated by nondimensional parameter k, based on the bending moment M_c at $\theta=\alpha/2$.

$$k=\frac{\sigma_m h^2 t_w}{\pi^2 D_w}=\frac{M_c}{I}\cdot\frac{h}{2}\cdot\frac{h^2 t_w}{\pi^2 D_w} \qquad (7)$$

In which σ_m=extreme fiber stress obtained by beam theory, I=moment of inertia of the beam.

3. NUMERICAL RESULTS

The cross section of curved girders in bending deforms as shown in Fig. 4. In this figure, rotational angle of the girder section is regarded as the angle between z-axis and the line connected the intersections of web and upper or lower flange. And flange rotation due to deformation is regarded as the angle which is the flange rotation corrected by rotational angle of the girder section. Then the web deflection due to deformation is regarded as the displacement of the web corrected by the r-displacement due to the girder rotation. In the following, flange rotation or web deflection due to deformation is simply called flange rotation or web deflection respectively (Fig. 4).

The example of the web deflection in the case of $z=11.45$, $GJ_f/D_wh=12.6$ is shown in Fig. 5. The web deflection at A and B in Fig. 5 are shown in Fig. 6 ($z=11.45$) and Fig. 7 ($z=1.72$). Fig. 6 (b) or Fig. 7 (b) shows the flange rotation at C in Fig. 5. In Fig. 7, the curve for $GJ_f/D_wh=1.58$, $EI_f/D_wh=1\,138$ is that for $A_{fc}/A_w=0.5$, others are for $A_{fc}/A_w=1.0$. In curves for $GJ_f/D_wh=12.6$, EI_f/D_wh is different because of the value of t_f and t_w.

In Fig. 6 and Fig. 7, thin lines indicate curves for the analytical model considered only web panel, and solid line and broken line indicate curves for fixed supported and simply supported models along flange-web connections respectively. In the following, for the simplicity, the models of only web panel are indicated by F. S. for fixed supported and S. S. for simply supported.

Fig. 8 shows the web deflection for $GJ_f/D_wh=12.6$ and $EI_f/D_wh=9\,100$. And Fig. 9 shows the web deflection for S. S.. In Fig. 6~Fig. 9, the buckling load of the web panel[2),17)] and torsional buckling load of compressive flange[15)] are shown. As torsional buckling of compressive flange, the buckling load is obtained as $k=73.7$ in Fig. 6 ($h/t_w=300$, $b/t_f=24$, $A_{fc}/A_w=1.0$) and $k=30.9$ in Fig. 7 ($h/t_w=150$, $b/t_f=16.7$, $A_{fc}/A_w=0.5$), because the value of bending moment is expressed by eq. (7), but the bending moment itself in Fig. 7 ($h/t_w=150$) is larger than that in Fig. 6 ($h/t_w=300$) when torsional buckling occurs.

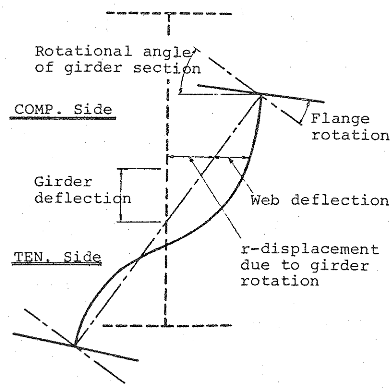

Fig. 4 Displacement and deformation of girder cross section.

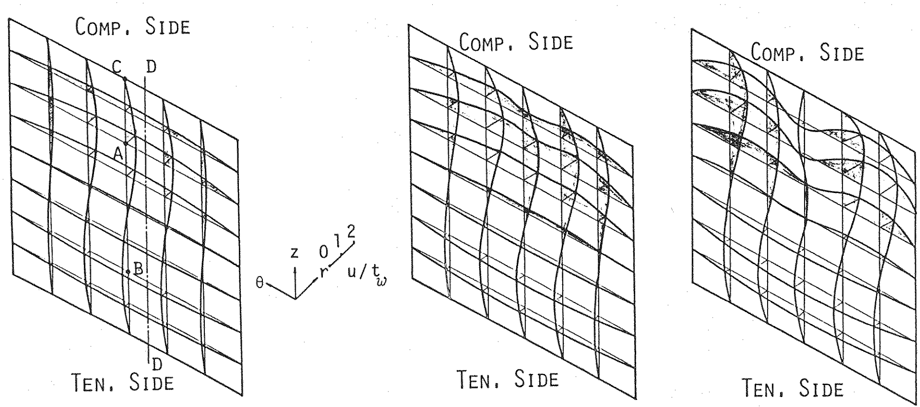

(a) $k=42$ (b) $k=85$ (c) $k=141$

Fig. 5 Web deflection ($z=11.45$, $GJ_f/D_wh=12.6$).

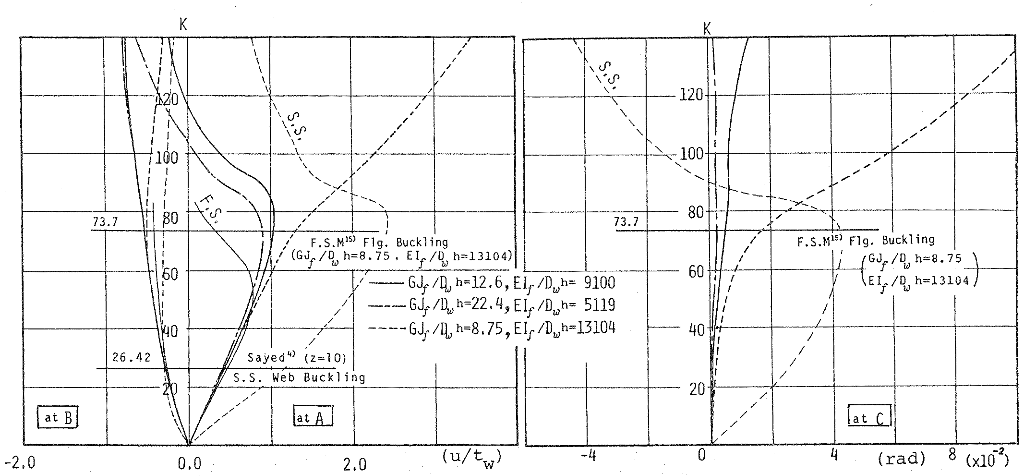

(a) Web deflection at A and B (b) Flange rotation at C

Fig. 6 Web deflection and flange rotation ($z=11.45$).

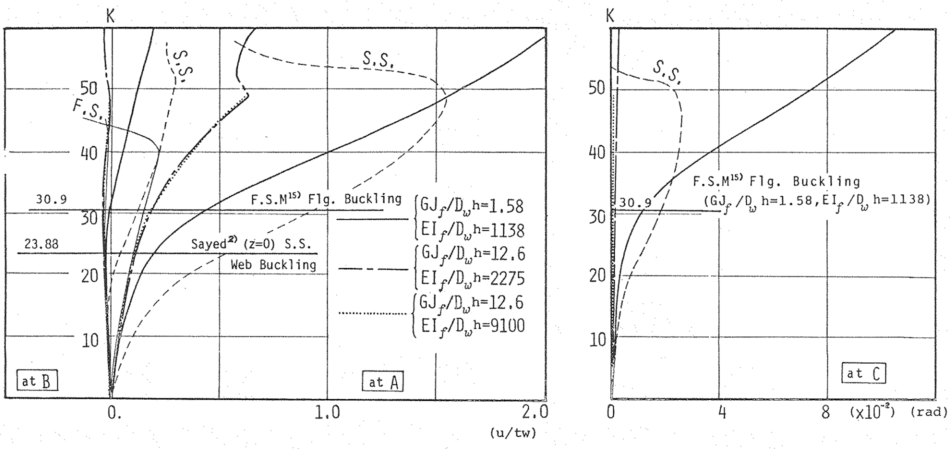

(a) Web deflection at A and B (b) Flange rotation at C

Fig. 7 Web deflection and flange rotation ($z=1.72$).

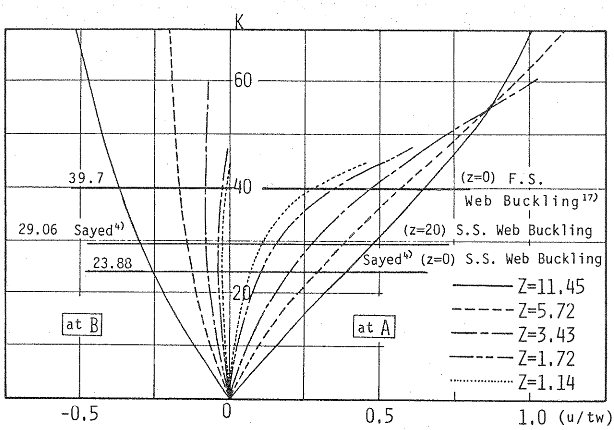

Fig. 8 Web deflection ($GJ_f/D_wh=12.6$, $EI_f/D_wh=9100$).

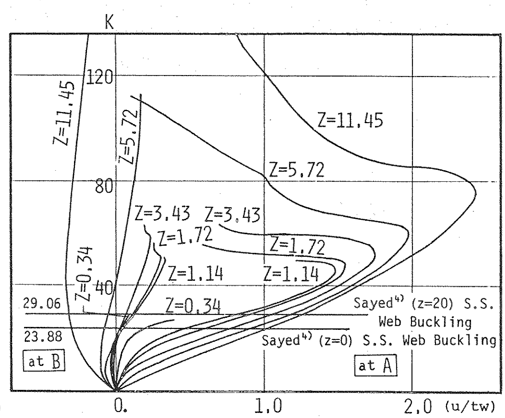

Fig. 9 Web deflection of cylindrical shell panel (S. S.).

These figures suggest as follows :

(1) when the load is small, the web deflects inward in the tension region (at B) and outward in the compressin region (at A). And the deflection of tension region does not become so large when the load increases.

(2) On the other hand, in the case $Ra/h=1$, the deflection of compression region of the web changes from a half wave of sinusoidal curve (1st-mode) to 1.5-waves (3 rd-mode) as shown in **Fig. 5**, when the load become large. Therefore, the deflection at A, as shown in **Fig. 6** or **Fig. 9**, decreases when the load reaches a certain value. These were also shown by Kuranishi&Hiwatashi[7].

(3) This phenomenon that the web deflection changes from 1st-mode to 3rd-mode appears obviously in the web panel model (**Fig. 9**) when z is larger than 1. But the model with flange panel is not so obvious without the case with large curvature ($z=11.45$). And, from **Fig. 6** (a), the load which the mode of the web deflection begins to change is larger than that in S. S. or F. S.. This suggests that the nonlinear behaviour of the flange which is rotated by compressive stresses acts to constrain the deflection mode of the web.

(4) In **Fig. 8**, the web deflections for $z<1.72$ increase remarkably at $k=39.7$ which is web buckling load for $z=0$ of F. S.. This phenomenon, which is called buckling phenomena of web panel in this paper, does not appear so obviously when $z>3$, but geometric nonlinearity appears clearly. And in **Fig. 9**, too,

buckling phenomena of the web panel are also noticed when $z<3$, but the phenemena become indistinctly as z becomes larger.

(5) When $Ra/h=1$, 2nd-mode deflection (a wave of sinusoidal curve) is obtained as eigen value problem, but in this analysis, 2nd-mode does not appear and 1st or 3rd mode is obtained.

(6) As for $GJ_f/D_wh=8.75$ in **Fig. 6** and $GJ_f/D_wh=1.58$ in **Fig. 7**, rotational angle of the compressive flange becomes large when k is larger than 73.7, 30.9 respectively, which are considered as torsional buckling loads of compressive flange. And the web deflection at A (compressive region) becomes visibly large.

(7) As shown in **Fig. 7**, EI_f/D_wh does not affect to the web deflection and GJ_f/D_wh gives the web deflection as in F. S. when the load is small.

(8) Summarizing previous discussions, so far as the load is small ($k<30$), the practical deformation is able to be approximately estimated by the analysis of web panel model which is assumed as F. S.. When the load becomes large, the web behaviour is remarkably affected by the phenomena of flange torsional buckling or geometrical nonlinear behaviour of compressive flange. Therefore, it is considered that the web panel model is inadequate to estimate the practical deformation of curved girders, and the analysis considered flange rigidities should be performed in the case of large load.

(2) Circumferential membrane stress

Fig. 10~**Fig. 12** show the distribution of circumferential membrane stresses on the cross section D-D in **Fig. 5**. The distribution of the stresses for each parameter z is shown in **Fig. 10**. The distribution of the stresses for $GJ_f/D_wh=12.6$ is compared with that of S. S. or F. S. in **Fig. 11**. **Fig. 12** shows the distribution of the stresses for each $b/t_f(GJ_f/D_wh)$. The curve for $GJ_f/D_wh=8.75$ in **Fig. 12**(a) and that for $GJ_f/D_wh=1.58$ in **Fig. 12**(b) indicate the distribution of the stresses by post-buckling of the

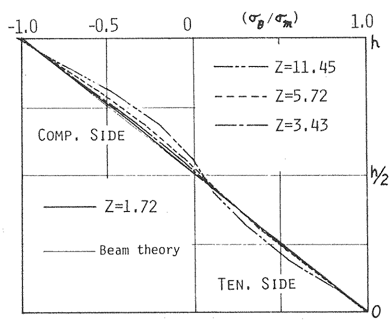

Fig. 10 Distribution of circumferential membrane stresses on section D-D in **Fig. 5** ($k=42.3$, $GJ_f/D_wh=12.6$, $EI_f/D_wh=9100$).

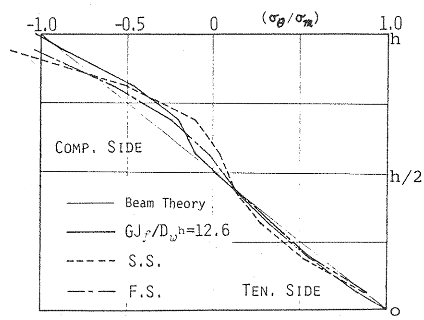

Fig. 11 Distribution of circmferential membrane stresses on section D-D in **Fig. 5** ($k=56.4$, $z=11.45$).

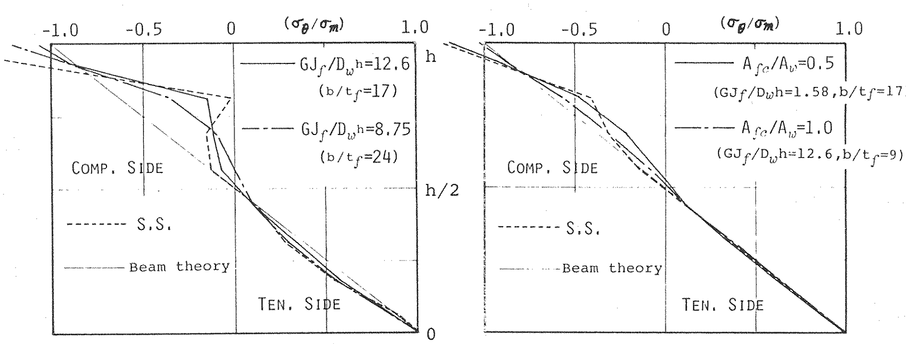

(a) $k=126.3$, $z=11.45$, $h/t_w=300$, $A_{fc}/A_w=1.0$

(b) $k=56.0$, $z=1.72$, $h/t_w=150$

Fig. 12 Distribution of circumferential membrane stresses on section D-D in **Fig. 5**.

compressive flange. Then, Table 1 (a), (b) show the extreme fiber stress of the web in compression region corresponding with Fig. 12(a), (b) respectively.

In these figures and table, membrane stress σ_θ is expressed by σ_θ/σ_m in which $\sigma_m (=M_c \cdot h/2I)$ indicate the extreme fiber stress based on beam theory. From these figures and tables, following discussions are developed :

(1) The membrane stresses in the compression region of the web are less than those based on beam theory. And the larger z or load becomes, the larger this reduction becomes.

(2) The membrane stresses in tension region of the web are less than those based on beam theory, too, when z becomes large. But this reduction is not so great as that in compression region.

(3) Fig. 10 shows that as for $z<2$, the difference between membrane stresses of this analysis and that based on beam theory is negligible when the load is small ($k<40$).

(4) Comparing the results of web panel model with those of plate and shell structure model (Fig. 11), the reduction of the membrane stresses at A shown in Fig. 5 is great in the order of F. S., the model of plate and shell and S. S.. This order corresponds to the web deflection at A shown in Fig. 7(a).

(5) The extreme fiber stress for web panel model is fairly larger than σ_m. However the extreme fiber stress considered flange ridigities is slightly larger than σ_m. This indicates that as for web panel model, the extreme fiber stress in the compression region must increase corresponding to the reduction of membrane stresses, while as for the model considering flange rigidities, web assignment of bending moment becomes less than that based on beam theory ($I_w/I, I_w=h^3 t_w/12$). Corresponding to this reduction of web assignment, the stresses of the compressive flange must increase.

(6) However, as shown in Fig. 10~Fig. 12, this stress increment of the compressive flange according to the reduction of the membrane stresses of web is small comparing with σ_m, and is at most $0.05\ \sigma_m$ as shown in Table 1(a), (b).

(7) Therefore, it is known that the increment of stresses of the compressive flange due to the stress reduction of the web is not a serious problem if A_{fc}/A_w is not extremely small. The stress increment for $A_{fc}/A_w=0.5$ is slightly greater than that for $A_{fc}/A_w=1.0$ as shown in Table 1(b).

(8) The extrme fiber stress for $GJ_f/D_w h=8.75 (b/t_f=24)$ in Fig. 12(a) is remarkably greater than σ_m. The same phenomena is observed for $GJ_f/D_w h=1.58 (b/t_f=17)$. This increment of the stress of the compressive flange is obviously caused by not the reduction of the web but phenomena of torsional buckling of the compressive flange as shown in Fig. 6 and Fig. 7, and is $0.2\ \sigma_m \sim 0.3\ \sigma_m$ as shown in Table 1, in which the stress for post-buckling of flange is indicated by the parenthesis.

4. SUMMARY AND CONCLUSIONS

The bending behaviour of curved girder-web was studied considering the rigidities of the flange panel.

Table 1 Circumferential compressive fiber stress in web panel (σ_θ/σ_m)

(a) $z=11.45$, $A_{fc}/A_w=1.0$

$GJ_f/D_w h$	22.4	12.6	8.75
k \ b/t_f	9	16.7	24
14.1	1.0187	1.0194	1.0227
49.4	———	———	1.0386
67.0	———	———	1.0484
77.6	1.0345	1.0381	(1.0655)
98.1	1.0392	1.0399	(1.1271)
110.1	1.0423	1.0440	(1.1668)
122.8	1.0470	1.0486	(1.2011)
133.4	1.0499	1.0517	(1.2308)

(b) $z=1.72$

A_{fc}/A_w	1.0	1.0	0.5
h/t_w	300	150	150
k \ $GJ_f/D_w h$	12.6	12.6	1.58
14.1	1.0005	1.0004	1.0004
24.7	1.0012	1.0010	1.0042
38.8	1.0038	1.0038	1.0491
48.0	1.0095	1.0100	(1.1186)
56.2	———	1.0252	(1.1900)
66.1	———	1.0365	(1.2726)

Results are obtained for the web deflection caused by girder deformations and the distributions of membrane stresses in the web, and are compared with results from web panel models of the previous investigations. Mereover the interaction of flange and web is discussed.

Based on the results of this study, the following conclusions seem to be warranted :

(1) When the deformation analysis is performed about the structural part between vertical stiffeners of curved girders, sectional forces and displacements at the end cross section of the analytical part should be compatible to the state of the practical curved girders. In this study, this compatibility is able to be satisfied by applying the assumption of displacement field of beams to the end cross sections.

(2) When the web aspect ratio $R\alpha/h=1$, and parameter z is large, the web deflection in compression region moves from 1st-mode to 3rd-mode as the bending moment increases. This phenomena appears eminently as for the web panel model of $z>1$. But as for the model considered flange panel, this phenomena does not appear so eminently as web panel models because the web behaviour is influenced by geometric nonlinearity of the flange panel.

(3) When $z<2$, the buckling phenomenon of the web is observed, and the circumferential membrane stresses are not so different from those based on beam theory. However when z is large, the buckling phenomenon of the web becomes indistinct, and the web deflections are largely affected by geometric nonlinearity as shell panel. Then, in this study, only 1st or 3rd mode of web deflection is obtained when $R\alpha/h=1$, although 2nd mode is obtained by eigen value problem in web bending buckling analysis.

(4) Depending on the reduction of membrane stresses of the web panel, the extreme fiber stress of the web in compression region becomes greater than that based on the beam theory. This is eminently observed in results of web panel model. But as for the model considered flange panel, the increment of compressive stresses of the flange is not so large, and is less than several percents of σ_m. Therfore, if A_{fc}/A_w is not extremely small, this increment of compressive stresses of flange is not a serious problem.

(5) However, if the phenomenon of torsional buckling of the compressive flange occurs, the web deflection in compression region increase rapidly. And the stresses of the compressive flange concentrate in the neighbourfood of flange-web connection, according to the stress reduction of the flange tip which is caused by the flange deflection. As the result, the extreme fiber stress of the web becomes greater 20 ~30 percents than that based on beam theory.

(6) When $GJ_f/D_wh=1.5\sim90$ and the load is small $(k<30)$, the deformation can approximately be evaluated by the analysis of web panel model in which the flange-web connection is assumed to be fixed. The sectional deformation is not affected so greatly by the value of EI_f/D_wh. However, the flange rigidities should be estimated in the large load case of the problem in the strength of curved girders, because the web behaviour is remarkably affected by the geometrical nonlinear behaviour of the flange when the load is large.

REFERENCES

1) The Japanese Road Association : The Japanese Specification for Highway Bridge, Feb., 1980.
2) Abdel-Sayed, G. : Curved webs under combined shear and normal stress, Proc. of ASCE, Vol. 99, No. ST3, 1973.
3) Dabrowski, R. and Wachowiak, J. : Stresses in thin cylindrical webs of curved plate girders, Proc. of Colloquium of Design of Plate and Box Girders for Ultimate Strength, London, 1971, IABSE, Vol. 11, 1972.
4) Culver, C. G., Dym, C. L. and Brogan, D. K. : Bending behavior of cylindrical web panels, Proc. of ASCE, Vol. 98, No. ST10, 1972.
5) Culver, C. G., Dym, C. L. and Uddin, T. : Web slenderness requirements for curved girders, Proc. of ASCE, Vol. 98, No. ST3, 1973.
6) Mikami, I., Furunishi, K. and Yonezawa H. : Nonlinear behavior of cylindrical web panels under bending Proc. of JSCE, No. 299, July, 1980.
7) Kuranishi, S. and Hiwatashi, S. : Elastic behavior of web plates of curved plate girders in bending, Proc. of JSCE, No. 315, Nov., 1981.
8) Cantin, G. and Clough, R. W. : A curved cylindrical shell, finite element, AIAA jour., Vol. 6, No. 6, 1968.

9) Megard, G. : Planar and curved shell elements, Finite Element Methods in Stress Analysis, ed. Holand, I. &K. bell, TAPIR, 1969.

10) For example, Zienkiewitcz, O. C. : The Finite Element Method 3rd ed., McGraw-Hill, 1977.

11) Nakai, H., Kitada, T. and Ohminami, R. : Experimental study on bending strength of web plate of horizontally curved girder bridges, Proc. of JSCE, No. 340, Dec., 1983.

12) Nakai, H., Muramatsu, S. Yoshikawa, N. Kitada, T. and Ohminami, R. : A Survey for web plates of the Horizontally Curved Girder Bridges, Bridge and Foundation, May, 1981.

13) Mikami I. and Furunishi, K. : Nonlinear behavior of cylindrical web panels under bending and shear, Proc. of the 29th Japan National Congress for Applied Mechanics, 1979, Vol. 29, University of tokyo Press., 1981.

14) The Task Committee on Curved Girder of the ASCE-AASHTO Committee on Flexural Members of the Committee of the Structural Division, Curved I-girder Bridge Design Recomendations, Proc. of ASCE, Vol. 103, No. ST5, 1977.

15) Fujii, K., Ohmura, H. and Kawano, Y. : Local buckilng analysis of curved girder flange by finite strip method, 35th Annual Conference of JSCE, Nov., 1980.

16) Fujii, K. and Ohmura, H. : Nonlinear Finite Element Analysis of curved Girder Deformation, Bulletin of Faculty of Engineering, Hiroshima Univ. Vol. 31, No. 1, 1983.

17) Handbook of Structural Stability, C. R. C. of Japan, Corona, June 1980.

18) Culver, C. G. and Frampton, R. E. : Loacal instability of holizontally curved members, Proc. of ASCE, Vol. 96, No. ST2, Feb., 1970.

(Received June 4 1984)